PPS
Paper
www.rsc.org/pps

Photoinduced electron transfer and electron-mediating systems from aromatic amines to triplet states of C_{60} and C_{70} in the presence of a viologen dication

Yoshiko Sasaki,[a,b] Yasuyuki Araki,[a] Mamoru Fujitsuka,[a] Osamu Ito,*[a] Akiko Hirao[c] and Hideyuki Nishizawa[c]

[a] *Institute of Multidisciplinary Research for Advanced Materials, Tohoku University, CREST, Japan Science and Technology Corporation (JST), Katahira, Sendai, 980-8577, Japan. E-mail: ito@tagen.tohoku.ac.jp*
[b] *Shokei Girl's High School, Hirose-machi, Aoba-ku, Sendai, 980-0873, Japan*
[c] *Research Development Center, Toshiba Corp. Komukai, Saiwai-ku, Kawasaki, 212-8582, Japan*

Received 17th September 2002, Accepted 6th November 2002
First published as an Advance Article on the web 6th January 2003

Photoinduced electron transfer between fullerenes (C_{60} and C_{70}) and various aromatic amines (AA's) in the absence and presence of a viologen dication has been studied by the transient absorption method in the visible and near-IR regions. Electron-transfer takes place from AA's to the triplet states of fullerenes ($^3C_{60}$* and $^3C_{70}$*) giving the anion radicals of fullerenes ($C_{60}^{\bullet -}$ and $C_{70}^{\bullet -}$) and the radical cations of AA's ($AA^{\bullet +}$). The rate constants and efficiencies of electron transfer are quite high, because of the high electron-donor abilities of AA's as their low oxidation potentials indicate. The absorption bands of $AA^{\bullet +}$ appeared also in the near-IR region indicating that the radical-cation center (hole) delocalizes over the entire region of each AA. On addition of an octylviologen dication (OV^{2+}) to C_{60}/C_{70}–AA systems, the electron-mediating process from $C_{60}^{\bullet -}$ and $C_{70}^{\bullet -}$ to OV^{2+} occurs yielding the viologen radical cation ($OV^{\bullet +}$) with longer lifetime.

Introduction

It has been pointed out that fullerenes (C_{60} and C_{70}) act as good electron acceptors in photoinduced electron-transfer processes.[1–4] Because of high delocalization of the π-electrons in C_{60} and C_{70}, the transient absorption bands due to the excited singlet states ($^1C_{60}$* and $^1C_{70}$*), triplet states ($^3C_{60}$* and $^3C_{70}$*), and anion radicals ($C_{60}^{\bullet -}$ and $C_{70}^{\bullet -}$) have been reported to appear in the near-IR region.[5,6] In addition, aromatic amines (AA's) with highly delocalized π-electron systems are useful for the charge-generating reagents and charge-mediating reagents in the electroluminescence devices, which attract much attention because of wide technological applications.[7] Absorption bands of the radical cations of such AA's with highly delocalized π-systems would be anticipated to appear at longer wavelengths. Thus, it is critical to measure the transient spectra in the visible and near-IR regions in order to disclose the routes and rates of the generations and movements of electrons and holes in the highly developed π-electron systems.

As routes of photoinduced electron-transfer processes of fullerenes in the presence of AA's, it has been reported that fullerenes in the excited states accept the electron from the electron-donors in their ground states.[8–10] The relative contributions of the singlet states and the triplet states of fullerenes to the photoinduced electron-transfer process vary with concentration of donors. Since the intersystem crossing processes (k_{isc}) from the singlet excited states to the triplet states of C_{60} and C_{70} are as fast as 10^9 s^{-1},[11,12] the excited singlet route can be achieved only at high concentrations of AA's; $k_{isc} < k_{et}^{S}$[AA], where k_{et}^{S} is the rate constant for electron transfer *via* the singlet excited states of C_{60} and C_{70}.[13,14] On the other hand, the triplet route is favorable at low concentrations of AA's; $k_{isc} > k_{et}^{T}$[AA], where k_{et}^{T} is the rate constant for electron transfer *via* the triplet excited states of C_{60} and C_{70}.[15,16]

We have reported that the efficiencies and rates of the photoinduced electron transfer can be evaluated by the transient absorption method in the visible and near-IR regions. From the decay of the excited states and the rise of the anion radicals of fullerenes in the presence of AA's, the rate parameters can be obtained.[9] In the present study, we employed AA's as shown in Scheme 1.[7,17] The π-conjugations in the AA moieties would be extended by the double bonds (butadiene (**1**), hydrazone (**2**) and ethylene (**4** and **7**)), biphenyl (**3**), oxadiazole (**5**) and pyrazole (**6**), which have been used as charge-generating and charge-transferring materials in the electroluminescence devices.[7,17] The rates and quantum yields for the electron-transfer processes *via* $^3C_{60}$* and $^3C_{70}$* were compared with changing the structures of AA's.

Furthermore, we investigate the addition effect of the viologen dication † (octylviologen dication, OV^{2+} was employed because of high solubility in polar organic solvents); in such systems, $C_{60}^{\bullet -}$ and $C_{70}^{\bullet -}$ can mediate their electrons to OV^{2+}. This reveals that an efficient photosensitizing electron-transfer–electron-mediating system will be established upon photoexcitation of fullerenes.

Results and discussion

Cyclic voltammetry

Cyclic voltammetry of these AA's in PhCN shows the reversible wave giving the first-oxidation potentials (E_{ox}), which are summarized in Table 1; **6** < **1** ≈ **2** < **7** < **3** < **4** ≈ **5**. Among these AA's, **6** shows the lowest E_{ox} value, suggesting a highly exothermic reaction with a large negative free-energy change in electron-transfer (ΔG°_{et}). Another low E_{ox} value was observed for **1**, which is a diene substituted with dialkylanilines; **7** also shows a low E_{ox} value as its molecular structure is similar to **1**. Aldehyde hydrazone (**2**) also has a low E_{ox} value. In **3**, the non-planarity of the biphenyl moiety gives an intermediate

† The IUPAC name for viologen dication is 4,4′-bipyridinium dication.

 DOI: 10.1039/b209111a

Table 1 Oxidation potentials (E_{ox}) of AA's and absorption maxima (λ_{max}) and molar absorption coefficients (ε_c) of radical cations of AA's in PhCN

AA's	E_{ox} [a]/V	Radical cations	λ_{max}/nm	ε_c [b]/mol^{-1} dm^3 cm^{-1}
1	0.057	**1**$^{\bullet+}$	850	7900
			600	21500
2	0.081	**2**$^{\bullet+}$	1070	11200
			920	31500
3	0.26	**3**$^{\bullet+}$	1300	16100
4	0.43	**4**$^{\bullet+}$	980	15000
5	0.41	**5**$^{\bullet+}$	1500	15300
6	−0.019	**6**$^{\bullet+}$	1280	14000
			620	22000
7	0.10	**7**$^{\bullet+}$	800	6700

[a] Values *vs.* Fc/Fc$^+$. [b] The ε_c values were evaluated on a comparison with that of $C_{70}^{\bullet-}$(4000 mol^{-1} dm^3 cm^{-1} at 1380 nm).[18]

E_{ox} value. Oxadiazole (**5**) shows the highest E_{ox} value among them.

Steady-state UV/visible spectra

These AA's are a faint yellow colour showing a strong absorption in a shorter wavelength region than 440 nm. On excitation of the AA's with the 532 nm laser light, appreciable transient absorption bands were not observed. Thus, it is presumed that the laser light at 532 nm predominantly excites C_{60}. To reveal the charge-transfer interaction, the steady-state absorption spectra of the mixture of C_{60}/C_{70} and the AA's were compared with the calculated spectrum by adding each spectrum of C_{60}/C_{70} and the AA's. Both spectra are almost the same, suggesting that no appreciable interaction exists between C_{60}/C_{70} and the AA's.

The steady-state absorption spectra of the radical cations of the AA's (AA$^{\bullet+}$'s) were observed by chemical oxidation with $FeCl_3$ in PhCN, as shown in Fig. 1. The absorption maxima

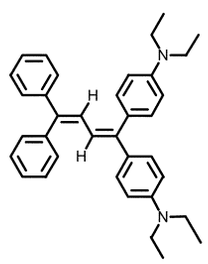

No. 1

1,1-bis{4-(*N*,*N*-diethylamino)phenyl}-4,4-diphenyl-1,3-butadiene

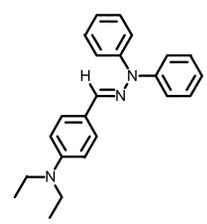

No. 2

4-(*N*,*N*-diethylamino)benzaldehyde diphenylhydrazone

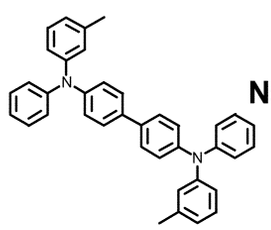

No. 3

4,4'-bis(*N*-phenyl-*N*-*m*-tolylamino)biphenyl

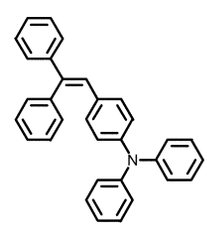

No. 4

N,*N*-diphenyl-*N*-{4-(2,2-diphenylethenyl)phenyl}amine

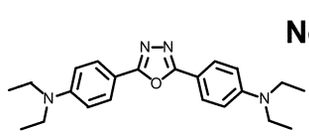

No. 5

2,5-bis{4-(*N*,*N*-diethylamino)-phenyl}-[1,3,4]oxadiazole

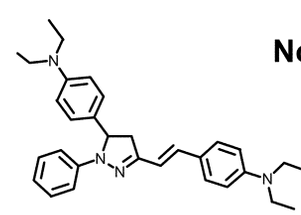

No. 6

4,5-dihydro-5-{4-(*N*,*N*-diethylamino)-phenyl}-3-[2-{4-(*N*,*N*-diethylamino)phenyl}ethenyl]-1-phenylpyrazole

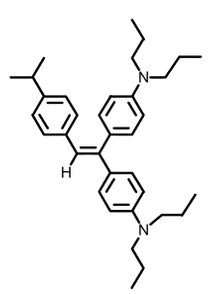

No. 7

1,1-bis{4-(*N*,*N*-diethylamino)phenyl}-2-(4-isopropylphenyl)ethene

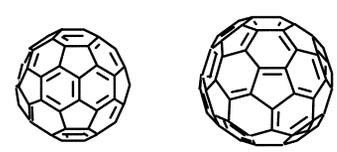

C_{60} C_{70}

Scheme 1 The molecular structures of AA's and fullerenes employed in the present study.

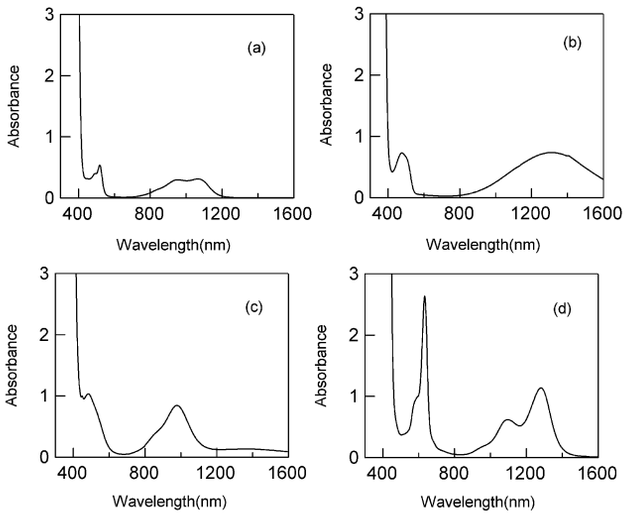

Fig. 1 Steady-state absorption spectra observed on addition of $FeCl_3$ to the AA's in PhCN; (a) **2**, (b) **3**, (c) **4**, and (d) **6**.

(λ_{max}) of the $AA^{\bullet+}$'s are summarized in Table 1, in which the molar absorption coefficients (ε_c) of $AA^{\bullet+}$'s were evaluated on the basis of the molar extinction coefficient of $C_{70}^{\bullet-}$ (ε_A = 4000 mol^{-1} dm^3 cm^{-1} at 1380 nm) observed by the laser flash photolysis as described in the next section.[18,19]

Transient absorption spectra and electron-transfer route

Nanosecond transient spectra observed by the laser excitation of C_{60} in the visible and near-IR regions in the presence of **6** in PhCN are shown in Fig. 2. The absorption band of $^3C_{60}$* at

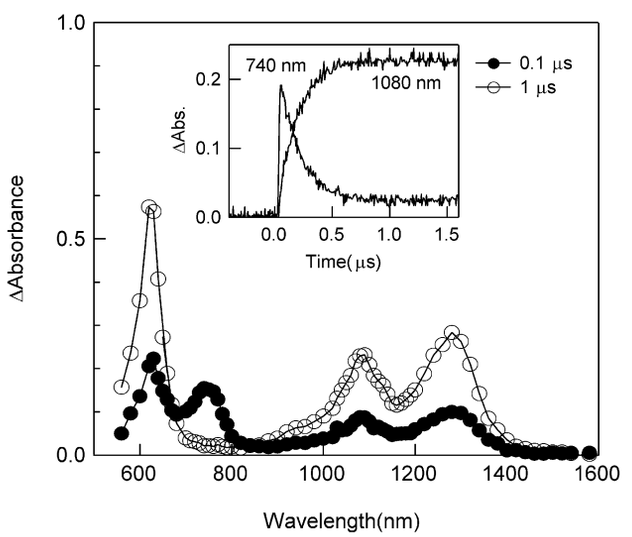

Fig. 2 Transient absorption spectra obtained by 532 nm laser light excitation of C_{60} (0.1×10^{-3} mol dm^{-3}) in the presence of **6** (1×10^{-3} mol dm^{-3}) in deaerated PhCN. Inset: time profiles at 740 and 1070 nm for the mixture of C_{60} (0.1×10^{-3} mol dm^{-3}) and **6** (1.0×10^{-3} mol dm^{-3}).

740 nm,[3–6] which appeared immediately after the laser exposure, began to decay in the presence of **6**. Concomitant with the decay of $^3C_{60}$*, the absorption intensity at 1080 nm increased, indicating that $C_{60}^{\bullet-}$ and $\mathbf{6}^{\bullet+}$ are formed *via* $^3C_{60}$* accepting an electron from **6**.[5,8–10] The absorption bands at 620 nm and 1280 nm appearing after the decay of $^3C_{60}$* can be attributed to $\mathbf{6}^{\bullet+}$ from the comparison with the steady-state absorption spectrum of $\mathbf{6}^{\bullet+}$ (Fig. 1d).

The time profiles for the decay of $^3C_{60}$* at 740 nm and the rises of $C_{60}^{\bullet-}$ and $\mathbf{6}^{\bullet+}$ at 1080 nm are shown in Fig. 2. The decay curve of $^3C_{60}$* and rise curves of $C_{60}^{\bullet-}$ and $\mathbf{6}^{\bullet+}$ are almost mirror images, supporting the conclusion that electron transfer

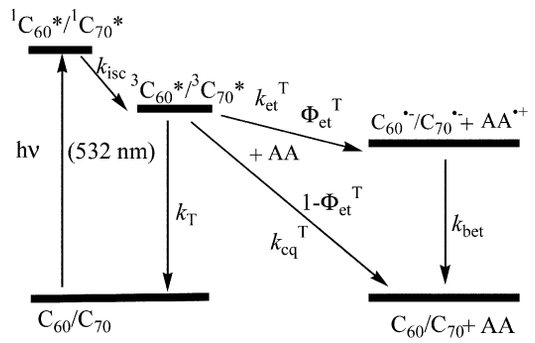

Scheme 2 Energy diagram for electron transfer *via* $^3C_{60}$*/$^3C_{70}$*.

takes place *via* $^3C_{60}$* as shown in Scheme 2, in which k_{isc}, k_{et}^T, k_{cq}^T, and k_{bet} are the rate constants of the intersystem crossing, electron transfer, collisional quenching, and back electron transfer, respectively. The observed slow rises of $C_{60}^{\bullet-}$ and $\mathbf{6}^{\bullet+}$ indicate clearly that electron transfer does not take place *via* $^1C_{60}$*.[14] The contribution of $^1C_{60}$* to the formations of the radical ions would be anticipated by further addition of the AA's; however, additions of the high concentration of the AA's to C_{60} in PhCN prohibited the observation of the radical ions, probably because of the formation of the exciplexes, which do not dissociate into the radical ions.

Each decay of $^3C_{60}$* at 740 nm obeys first-order kinetics (Fig. 2), yielding the first-order rate constant (k_{1st}). In the absence of the AA's, the k_{1st} value can be made equal to k_T which is 10^4 s^{-1}. The k_{1st} value increases linearly with the concentration of the AA donor. In the presence of the AA's, k_{1st} is in the order of 10^6–10^7 s^{-1}. The second-order quenching rate constants (k_q^T) of $^3C_{60}$* by the AA donors can be obtained from the slopes of the pseudo-first-order plots as listed in Table 2. These k_q^T values do not vary much with changing AA's, falling in a narrow range of (2.4–4.0) $\times 10^9$ mol^{-1} dm^3 s^{-1}. These values are close to the diffusion controlled limit ($k_{diff} = 5.2 \times 10^9$ mol^{-1} dm^3 s^{-1} in PhCN).[20]

The transient absorption spectra of C_{70} in the presence of **1** are shown in Fig. 3. The transient absorption band of $^3C_{70}$*

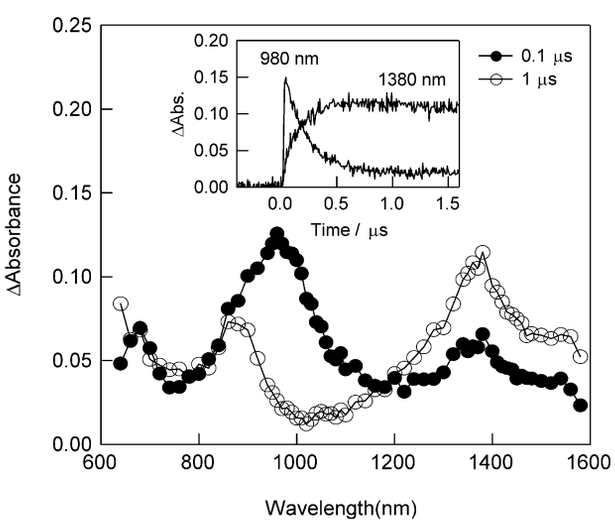

Fig. 3 Transient absorption spectra obtained by 532 nm laser light of C_{70} (0.1×10^{-3} mol dm^{-3}) in the presence of **1** (1×10^{-3} mol dm^{-3}) in PhCN. Inset: time profiles at 980 and 1380 nm.

at 940–980 nm appeared immediately after the laser-light exposure; then the absorption intensity of $C_{70}^{\bullet-}$ at 1380 nm increased after 1.0 μs. The observed time-profiles of the absorption bands of $^3C_{70}$* and $C_{70}^{\bullet-}$ are quite similar to those in Fig. 2. Since the rise rate of $C_{70}^{\bullet-}$ is similar to the decay rate of $^3C_{70}$*, $C_{70}^{\bullet-}$ is produced *via* $^3C_{70}$* accepting an electron from **1**. The k_q^T values are summarized in Table 2. The order of the k_q^T

Table 2 Free-energies (ΔG°_{et}), rate constants for quenching (k_q^T), quantum yields (Φ_{et}^T), rate constants (k_{et}^T) for electron-transfer from $^3C_{60}$* and $^3C_{70}$* to the AA's, and back electron-transfer rate constants (k_{bet}) from $C_{60}^{\bullet-}/C_{70}^{\bullet-}$ to the $AA^{\bullet+}$ in PhCN

AA donors	Fullerene acceptors	ΔG°_{et}/kJ mol^{-1}	k_q^T [a]/mol^{-1} dm^3 s^{-1}	Φ_{et}^T	k_{et}^T/mol^{-1} dm^3 s^{-1}	k_{bet} [b]/mol^{-1} dm^3 s^{-1}
1	C_{60}	−13.9	4.0×10^9	0.56	2.2×10^9	8.9×10^9
1	C_{70}	−13.5	3.3×10^9	0.30	9.9×10^8	3.2×10^9
2	C_{60}	−13.4	3.8×10^9	0.70	2.7×10^9	7.2×10^9
2	C_{70}	−12.9	7.7×10^9	0.80	6.2×10^9	6.8×10^9
3	C_{60}	−9.24	3.3×10^9	0.36	1.2×10^9	6.9×10^9
3	C_{70}	−8.78	2.4×10^9	0.51	1.2×10^9	4.5×10^9
4	C_{60}	−5.31	2.8×10^9	0.27	7.6×10^8	8.5×10^9
4	C_{70}	−4.85	4.6×10^9	0.19	8.7×10^8	4.7×10^9
5	C_{60}	−5.78	2.6×10^9	0.65	1.7×10^9	7.9×10^9
5	C_{70}	−5.31	3.3×10^9	0.70	2.3×10^9	7.1×10^9
6	C_{60}	−15.7	3.6×10^9	0.97	3.5×10^9	4.0×10^9
6	C_{70}	−15.2	1.8×10^9	0.70	1.3×10^9	2.5×10^9
7	C_{60}	−12.9	2.4×10^9	0.78	1.9×10^9	8.6×10^9
7	C_{70}	−12.4	4.6×10^9	0.71	3.3×10^9	4.3×10^9

[a] The k_q^T values for C_{60} were evaluated from the decay of $^3C_{60}$*, while the k_q^T values for C_{70} were evaluated from the rise of decay of $C_{70}^{\bullet-}$; both values contain error estimation of about 5%. [b] The k_{bet} values were evaluated using the ε_c values in Table 1; each k_{bet} value contains an estimation error of about 5%.

values for the C_{70}–AA systems is; **6** < **3** < **1** = **5** < **4** = **7** < **2**, in which the range of the values [(1.8–7.7) × 10^9 mol^{-1} dm^3 s^{-1}] is wider than that of the C_{60}–AA systems.

Quantum yields and rate constants for electron transfer

In the case of the C_{70}–AA systems, the efficiency of electron transfer *via* $^3C_{70}$* can be obtained from the ratio of the initial maximal absorbance of $^3C_{70}$* at 980 nm to the maximal absorbance of $C_{70}^{\bullet-}$ at 1380 nm, $[C_{70}^{\bullet-}]_{max}/[^3C_{70}*]_{int}$. As shown in Fig. 4, such ratios show saturation with an increasing

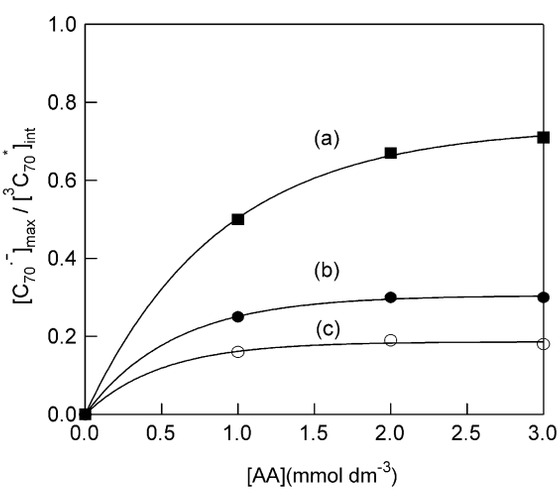

Fig. 4 Plots of efficiencies of electron transfer $[C_{70}^{\bullet-}]_{max}/[^3C_{70}*]_{int}$ *vs.* [AA]; (a) **7**, (b) **1**, and (c) **4**.

concentration of AA donors. At a sufficiently high concentration of AA donors above *ca.* 3 × 10^{-3} mol dm^{-3}, the efficiency can be made equal to the quantum yield (Φ_{et}) of the electron transfer process *via* $^3C_{70}$* (Table 2).[16,18] When the absorption band of $C_{70}^{\bullet-}$ was overlapping with the bands of $AA^{\bullet+}$, the absorbance due to $AA^{\bullet+}$ was subtracted using the ε_c values in Table 1. The observed order of Φ_{et} is **4** < **1** < **3** < **5** = **6** < **7** < **2**.

In the case of C_{60}–AA systems, the Φ_{et} values were similarly evaluated after subtraction of the absorbance of the radical cation from the absorbances of $^3C_{60}$* and $C_{60}^{\bullet-}$. The observed order of Φ_{et} is **4** < **3** < **1** < **5** < **2** < **7** < **6**. Since all Φ_{et} values in Table 2 are less than 1.0, there are quenching processes other than electron transfer in Scheme 2, these processes are described as collisional quenching processes, which may include deactivation *via* encounter complexes ($^3C_{60}$*/$^3C_{70}$* ··· AA) and exciplexes [$^3(C_{60}^{\delta-}/C_{70}^{\delta-}$ ··· $AA^{\delta+})$*] without forming the radical ions which persist more than *ca.* 10 ns.

Finally, the electron-transfer rate constants (k_{et}^T) can be obtained from the relation of $k_{et}^T = \Phi_{et}^T k_q^T$ as listed in Table 2.[16,18] Thus, the k_{et}^T values in the range of order of (7.6 × 10^8–6.2 × 10^9) mol^{-1} dm^3 s^{-1} were evaluated; these are slightly smaller than k_{diff} in PhCN.[20] The order of the obtained k_{et}^T values is **4** < **3** < **5** < **7** < **1** < **2** < **6** for C_{60}; this order reflects the order of Φ_{et}^T rather than that of k_q^T. For C_{70}, the order of the obtained k_{et}^T values is **4** < **1** < **3** < **6** < **5** < **7** < **2**; this order reflects both orders of Φ_{et}^T and k_q^T.

The ΔG°_{et} *via* $^3C_{60}$*/$^3C_{70}$* can be calculated from the E_{ox} of the AA's, reduction potentials (E_{red}) of C_{60}/C_{70}, and the energy level of the excited triplet state (E_T) of C_{60}/C_{70} according to Rehm-Weller equation (1):[21]

$$\Delta G^\circ_{et} = E_{ox} - E_{red} - E_T - E_c \qquad (1)$$

Here, E_T values (1.53 eV for $^3C_{60}$* and 1.50 eV for $^3C_{70}$*),[22,23] E_{red} values (−0.92 V *vs.* Fc/Fc^+ in PhCN for C_{60} and −0.93 V *vs.* Fc/Fc^+ in PhCN for C_{70}),[24,25] the E_{ox} of AA's (Table 1) and the Coulomb energy (E_c = 0.06 eV in PhCN)[5] were employed. The ΔG°_{et} values listed in Table 2 are all sufficiently negative to support the nearly diffusion-controlled rate constants for the electron-transfer processes. The order of these $-\Delta G^\circ_{et}$ values is **6** > **1** ≈ **2** > **7** > **3** > **4** > **5**, which reflects the order of the E_{ox} values of the AA's. However, these orders are not always similar to those of Φ_{et}^T and k_{et}^T. Factors other than ΔG°_{et} may control the orders of Φ_{et}^T and k_{et}^T, although such factors are not clarified in the present stage.

Back electron transfer process

In the longer time measurements, $C_{70}^{\bullet-}$ begins decaying after reaching the maximum intensity, as shown in Fig. 5 in a longer time scale. The second-order plot (1/ΔAbs. *vs.* time) for the decay of $C_{70}^{\bullet-}$ shows a linear relation in the initial stage (inset of Fig. 5); the later stage may contain a lot of noise. Observed second-order kinetics indicates a bimolecular reaction, probably by recombination of $C_{70}^{\bullet-}$ with $\mathbf{5}^{\bullet+}$ in the same concentration, yielding neutral molecules in their ground states (in Scheme 2). The bimolecular second-order kinetics also suggests that the back electron transfer takes place after the radical cation and radical anion were separately solvated as free radical ions. The slope of the second-order plot is attributed to k_{bet}/ε_A. On substituting the reported ε_A at 1380 nm for $C_{70}^{\bullet-}$, one can calculate the k_{bet} values as listed in Table 2. In the case of $C_{60}^{\bullet-}$, the k_{bet} values were similarly evaluated from the decays of the radical cations of AA's using the ε_c values listed in Table 1, because of overlapping of the absorption band of $C_{60}^{\bullet-}$ with those of $AA^{\bullet+}$. The k_{bet} values for $C_{60}^{\bullet-}$ are almost the same as

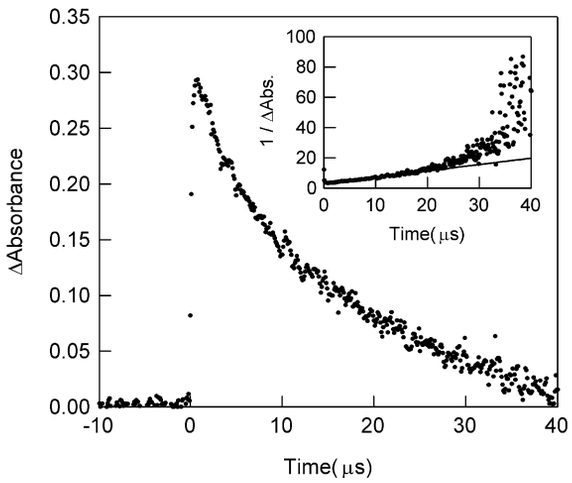

Fig. 5 Long time-scale decay of $C_{70}^{\bullet -}$ at 1380 nm produced by electron transfer from **5** in PhCN. Inset: second-order plot.

those of $C_{70}^{\bullet -}$. They are in the range of (2.5–8.9) × 10^9 mol^{-1} dm^3 s^{-1}, which are all quite near to the k_{diff} value in PhCN. Although $k_{bet} > k_{et}$, the rate of the forward reaction is faster than that of the backward reaction, because the concentration of the AA is much higher than that of the $AA^{\bullet +}$, even though the concentration of $C_{60}^{\bullet -}$ ($C_{70}^{\bullet -}$) is similar to that of $^3C_{60}$* ($^3C_{70}$*).

Electron-mediating system

On addition of the octylviologen dication (OV^{2+}) to the mixture of C_{60} and **5**, the transient absorption spectra were observed by the laser light excitation of C_{60}; these are shown in Fig. 6. Along

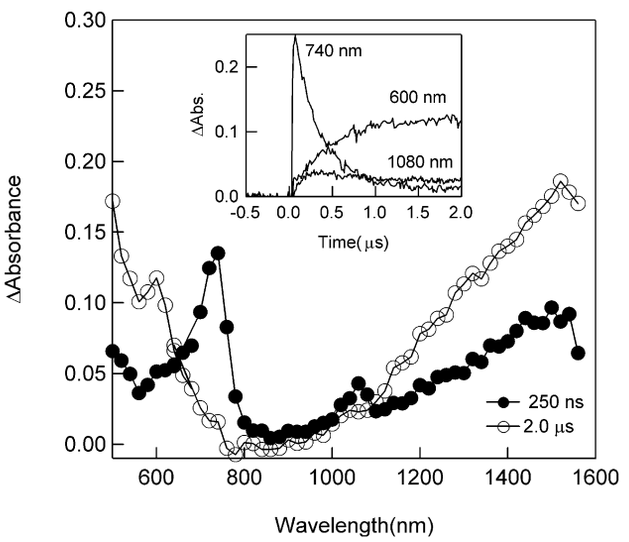

Fig. 6 Transient absorption spectra obtained by 532 nm laser light excitation of C_{60} (0.1 × 10^{-3} mol dm^{-3}) in the presence of **5** (1 × 10^{-3} mol dm^{-3}) and OV^{2+} (1 × 10^{-3} mol dm^{-3}) in PhCN. Inset: time profiles at 740, 1080, and 600 nm.

with the rapid decay of $^3C_{60}$* and the corresponding rapid rises of $C_{60}^{\bullet -}$ (1000–1100 nm) and $\mathbf{5}^{\bullet +}$ (1200–1600 nm), $OV^{\bullet +}$ appeared at 600 nm. At 600 nm, since the absorption band of $^3C_{60}$* may be overlapped, there is a small initial intensity in the rise profile at 600 nm in Fig. 6. The rise rate of $OV^{\bullet +}$ was almost the same as $C_{60}^{\bullet -}$ decay, as shown in Fig. 6. These observations suggest that $OV^{\bullet +}$ is produced by transferring an electron from $C_{60}^{\bullet -}$ to OV^{2+}, which is referred to as the electron-mediating process.[9] The E_{red} of OV^{2+} (−0.81 V *vs.* Fc/Fc^+ in PhCN) also suggests that this process irreversibly occurs, because this reaction is *ca.* 0.12 eV exothermic. Although $C_{60}^{\bullet -}$ should decay with the rise of $OV^{\bullet +}$, the time-profile of the 1080 nm band in the inset of Fig. 6 did not show clear decay, because the absorption of $\mathbf{5}^{\bullet +}$ overlapped with that of $C_{60}^{\bullet -}$ at 1080 nm; during the electron-mediating process, the absorption intensity of $\mathbf{5}^{\bullet +}$ does not vary. In the case of the C_{70}–AA–OV^{2+} system, the rise of $OV^{\bullet +}$ was observed after the electron transfer from the AA's to $^3C_{70}$*. Thus, the photosensitized electron-transfer–electron-mediating system was established with the photoexcitation of fullerenes (C_{60}/C_{70}) as shown in Scheme 3, in which k_{md} and k_{fbet}

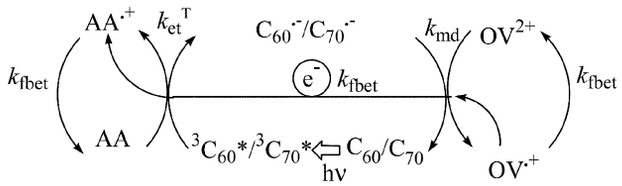

Scheme 3 Electron-mediating system.

are the rate constants of the electron-mediating process and of the final back electron-transfer process from $OV^{\bullet +}$ to $AA^{\bullet +}$, respectively. The k_{md} value was evaluated to be 2.8 × 10^9 mol^{-1} dm^3 s^{-1} in PhCN from the rise of $OV^{\bullet +}$ by changing the concentration of OV^{2+}.

In the longer time-scale measurements, the decay time-profiles of $\mathbf{2}^{\bullet +}$ at 920 nm in the presence and absence of OV^{2+} were observed as shown in Fig. 7. The decay rate of $\mathbf{2}^{\bullet +}$ in the

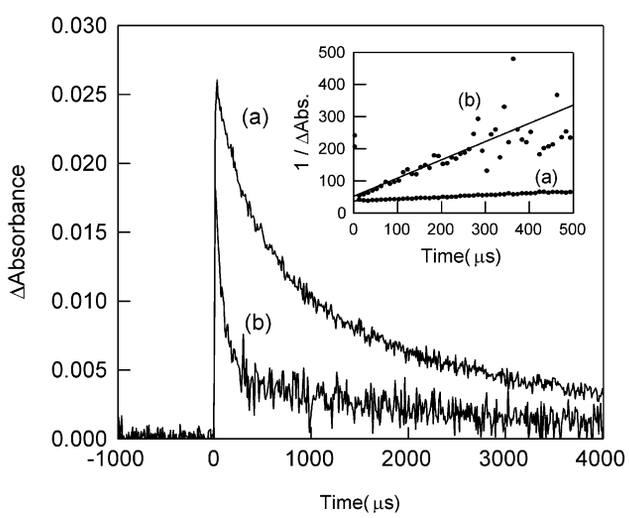

Fig. 7 Long time-scale decays of $\mathbf{2}^{\bullet +}$ at 920 nm produced *via* $^3C_{60}$* in PhCN; (a) in the presence of OV^{2+} and (b) in the absence of OV^{2+}. Inset: second order plots.

presence of OV^{2+} is slower than that in the absence of OV^{2+}. The slope of the second-order plot of $\mathbf{2}^{\bullet +}$ (or $OV^{\bullet +}$) gave k_{fbet} = 7.2 × 10^8 mol^{-1} dm^3 s^{-1}, while the slope in the absence of OV^{2+} gave k_{bet} = 7.2 × 10^9 mol^{-1} dm^3 s^{-1} (Table 2). This finding indicates that the lifetime of $\mathbf{2}^{\bullet +}$ in the presence of $OV^{\bullet +}$, which implies the absence of $C_{60}^{\bullet -}$, becomes longer compared with the back electron-transfer process between oppositely charged species $\mathbf{2}^{\bullet +}$ and $C_{60}^{\bullet -}$, suggesting that the rate of the electron-transfer process between the positively charged species ($\mathbf{2}^{\bullet +}$ and $OV^{\bullet +}$) slows down due to the repulsion.

Summary

In the present study, we have shown that C_{60} and C_{70} act as good photosensitizing electron acceptors in the presence of AA donors. Their transient species, such as triplet excited states and ion radicals, were well chased by the transient absorption spectra in the near-IR regions, although accidental overlapping of the absorption band of $C_{60}^{\bullet -}$ with $AA^{\bullet +}$ made it difficult to analyze the rates and efficiency of electron transfer. The delocalization of radical-cation centers (holes) was elucidated

from their near-IR bands. On addition of a viologen dication, the photosensitizing electron-transfer–electron-mediating cycle was established, producing prolonged lifetimes of the holes of AA's.

Experimental

Materials

C_{60} and C_{70} were obtained from Texas Fullerenes Corporation at a purity of 99.9 and 99%, respectively. The aromatic amines (AA's) employed in the present study were all available from Anan Koryo Ltd, Japan and Inui Regents Ltd, Japan. The Octylviologen dication (OV^{2+}) was obtained as a perchlorate salt. The PhCN used as solvent was of HPLC grade.

Apparatus

Oxidation potentials (E_{ox}) of AA's were measured by a voltammetric analyzer (BAS CV-50 W) in a conventional three electrode-cell equipped with Pt-working and counter electrodes with an Ag/Ag^+ reference electrode at scan rate of 100 mV s^{-1}. E_{ox} values in Table 1 are listed as Fc/Fc^+ standard. In each case, the solution of a sample with 0.1 mol dm^{-3} of tetrabutylammonium perchlorate (Nakalai Tesque) as electrolyte was deaerated with Ar-bubbling before measurements.

Steady-state absorption spectra were measured with a JASCO/V-570 spectrophotometer. The absorption spectra of the radical cations of the AA's were observed by the step-wise addition of $FeCl_3$ to the AA solutions.[9]

Transient absorption spectra in the visible and near-IR regions were observed by the laser-flash photolysis apparatus. In the systems of C_{60}/C_{70}–AA's and C_{60}/C_{70}–AA–OV^{2+}, C_{60} and C_{70} were excited with the SHG (532 nm) light of a Nd:YAG laser (Quanta-Ray; 6 ns fwhm). For shorter time-scale measurements than 10 μs, a Si-PIN photodiode module (400–600 nm) and a Ge-APD module (600–1600 nm) were employed as detectors for monitoring the light from a pulsed Xe-lamp.[19,20] For longer time-scale measurements than 10 μs, an InGaAs-PIN photodiode was used as a detector for monitoring light from a continuous Xe-lamp (150 W).[26,27] The sample solutions were deaerated by bubbling with argon gas before measurements. The laser photolysis was performed for the solution in a rectangular quartz cell with a 10 mm optical path. All the measurements were carried out at 23 °C. Details of the experimental procedures are described elsewhere.[19,20]

Acknowledgements

The authors are grateful to a financial supports by a Grant-in-Aid on Scientific Research from the Ministry of Education, Culture, Sports, Science, and Technology of Japan and by the Mitsubishi Foundation.

References

1 C. S. Foote, *Physics and Chemistry of the Fullerenes*, ed. K. Prassides, NATO ASI Series, vol. C-443, Kluwer Academic Publisher, Dordrecht, 1994, 79–96.
2 O. Ito, Photoinduced electron transfer of fullerenes (C_{60} and C_{70}) studied by transient absorption measurements in near-IR region, *Res. Chem. Intermed.*, 1997, **23**, 389–402.
3 M. Maggini and D. M. Guldi, *Molecular and Supramolecular Photochemistry*; ed. V. Ramamurthy andK. S. Schanze, Marcel Dekker, New York, 2000, vol. 4, pp. 149–196.
4 D. M. Guldi and P. V. Kamat, *Fullerenes, Chemistry, Physics and Technology*, ed. K. M. Kadish and R. S. Ruoff, Wiley-Interscience, New York, 2000, pp. 225–281.
5 J. W. Arbogast and C. S. Foote, Photophysical properties of C_{70}, *J. Am. Chem. Soc.*, 1991, **113**, 8886–8889.
6 R. J. Senior, A. Z. Szarka, G. R. Smith and R. M. Hochstrasser, Ultrafast photoinduced electron transfer to C_{60}, *Chem. Phys. Lett.*, 1991, **185**, 179–183.
7 M. Pope and C. E. Swenberg, *Electronic Processes in Organic Crystals and Polymers*, second edn., Oxford University Press, New York, 1999, pp. 1182–1229.
8 S. Fukuzumi, T. Suenobu, M. Patz, T. Hirasaka, S. Itoh, M. Fujitsuka and O. Ito, Selective one-electron and two-electron reduction of C_{60} with NADH and NAD dimer analogues *via* photoinduced electron transfer, *J. Am. Chem. Soc.*, 1998, **120**, 8060–8068.
9 O. Ito, Y. Sasaki, M. E. El-Khouly, Y. Araki, M. Fujitsuka, A. Hirao and H. Nishizawa, Photoinduced electron transfer from aromatic aldehyde hydrazones to triplet states of C_{60} and C_{70}; electron-mediating and hole-shifting systems, *Bull. Chem. Soc. Jpn.*, 2002, **75**, 1247–1254.
10 H. Onodera, Y. Araki, M. Fujitsuka, S. Onodera, O. Ito, F. Bai, M. Zheng and J.-L Yang, Photoinduced electron-transfer from mono-/oligo-1,4-phenylenevinylenes containing aromatic amines to C_{60}/C_{70} and electron-mediating process to viologen dication in polar solution, *J. Phys. Chem. A*, 2001, **105**, 7341–7349.
11 M. Gevaert and P. V. Kamat, Photochemistry of fullerenes: excited-state behavior of C_{60} and C_{70} and their reduction in poly(methyl methacrylate)films, *J. Phys. Chem.*, 1992, **96**, 9883–9888.
12 A. Watanabe, O. Ito, M. Watanabe, H. Satio and M. Koishi, Excited states of C_{70} and the intersystem crossing process studied by picosecond time-resolved spectroscopy in the visible and near-IR region, *J. Phys. Chem.*, 1996, **100**, 10518–10522.
13 J. Park, D. Kim, Y. D. Suh and S. K. Kim, Comparative study on photoinduced electron transfer from *N,N*-dimethylaniline (DMA) and 4,4′-methylenebis(*N*,*N*-dimethylaniline) (BDMA) to C_{60} and C_{70} in toluene, *J. Phys. Chem.*, 1994, **98**, 12715–12719.
14 H. N. Ghosh, H. Pal, A. V. Sapre and J. P. Mittal, Charge recombination reactions in photoexcited fullerene C_{60}-amine complexes studied by picosecond pump & probe spectroscopy, *J. Am. Chem. Soc.*, 1993, **115**, 11722–11727.
15 J. W. Arbogast, C. S. Foote and M. Kao, Electron transfer to triplet C_{60}, *J. Am. Chem. Soc.*, 1992, **114**, 2277–2279.
16 C. A. Steren, H. von Willigen, L. Biczok, N. Gupta and H. Linschitz, C_{60} as a photocatalyst of electron-transfer processes: Reactions of triplet C_{60} with chloranil, perylene, and tritolylamine studied by flash photolysis and FT-EPR, *J. Phys. Chem.*, 1996, **100**, 8920–8926.
17 S. Nomura and Y. Shirota, Concentration dependence of the activation energy for the hole drift mobility of 9-ethylcarbazole-3-carbaldehyde diphenylhydrazone dispersed in polycarbonate, *Chem. Phys. Lett.*, 1997, **268**, 461–464.
18 M. M. Alam, A. Watanabe and O. Ito, Electron transfer from tetrathiafulvalenes to photoexcited C_{70} studied by observing transient absorption in the near-IR region, *Bull. Chem. Soc. Jpn.*, 1997, **70**, 1833–1838.
19 M. M. Alam, O. Ito, N. Sakurai and H. Moriyama, Photoinduced electron transfer between fullerenes (C_{60}/C_{70}) and ethylene-dithiotetrathiafulvalene, *Res. Chem. Intermed.*, 1999, **25**, 323–338.
20 S. l. Murov, I. Carmichael and G. L. Hug, *Handbook of Photochemistry*, 2nd edn., Marcel Dekker, New York, 1993.
21 S. Fukuzumi and H. Imahori, in *Electron Transfer in Chemistry*, ed. V. Balzani, Wiley-VCH, Weinhaime, 2002, 927–975.
22 R. R. Hung and J. J. Grabowski, A precise determination of the triplet energy of carbon (C_{60}) by photoacoustic calorimetry, *J. Phys. Chem.*, 1991, **95**, 6073–6075.
23 R. E. Haufler, J. Conceicao, L. P. F. Chibante, Y. Chai, N. E. Byrne, S. Flanagan, M. M. Haley, S. C. O'Brien, C. Pan, Z. Xiao, W. E. Billups, M. A. Ciufolini, R. H. Hauge, J. L. Margrave, L. J. Wilson, R. Curl and R. E. Smally, Efficient production of C_{60}(buckminsterfullerene), $C_{60}H_{36}$, and the solvated buckide ion, *J. Phys. Chem.*, 1990, **94**, 8634–8636.
24 P. M. Allemand, A. Koch, F. Wudl, Y. Rubin, F. Diederich, M. M. Alvarez, S. J. Anz and R. L. Whetten, Two different fullerenes have the same cyclic voltammetry, *J. Am. Chem. Soc.*, 1991, **113**, 1050–1051.
25 D. Dubois, K. M. Kadish, S. Flanagan, R. E. Haufler, L. P. F. Chibante and L. J. Wilson, Spectroelectrochemical study of the C_{60} and C_{70} fullerenes and their mono-, di-, tri- and tetraanions, *J. Am. Chem. Soc.*, 1991, **113**, 4364–4366.
26 K. Matsumoto, M. Fujitsuka, T. Sato, S. Onodera and O. Ito, Photoinduced electron transfer from oligothiophenes/polythiophene to fullerenes (C_{60}/C_{70}) in solution; comprehensive study by nanosecond laser flash photolysis method, *J. Phys. Chem.*, 2000, **104**, 11632–11638.
27 T. Konishi, M. Fujitsuka, O. Ito, Y. Toba and Y. Usui, C_{60} as photosensitizing electron-transfer mediator for ion-pair charge-transfer complexes between borate anions and methyl viologen dication, *J. Phys. Chem. A*, 1999, **103**, 9938–9942.